

Article

Experimental Study on Thermal Management of 5S7P Battery Module with Immersion Cooling Under High Charging/Discharging C-Rates

Le Duc Tai, Kunal Sandip Garud  and Moo-Yeon Lee *

Department of Mechanical Engineering, Dong-A University, 37 Nakdong-Daero 550, Saha-gu, Busan 49315, Republic of Korea; 2377988@donga.ac.kr (L.D.T.); 1876936@donga.ac.kr (K.S.G.)

* Correspondence: mylee@dau.ac.kr; Tel.: +82-51-200-7642

Abstract: In this study, the efficiency of an immersion cooling system for controlling the temperature of 5S7P battery modules at high charge and discharge C-rates was experimentally evaluated. The study was conducted in three main stages including the evaluation of different coolant oils followed by the proposition of an optimal volume flow rate (VFR) and cooling performance evaluation under high charging/discharging C-rates. In the first stage, three coolant oils, including Therminol D-12, Pitherm 150B, and BOT 2100, were compared. The Therminol D-12 achieved superior cooling performance, with the highest heat transfer coefficient (HTC) of $2171.93 \text{ W/m}^2\cdot\text{K}$ and the ability to maintain the maximum temperature (T_{\max}) and temperature difference (ΔT) of the battery module within the safe range. In the next stage, VFR was varied between 0.4 LPM and 1.0 LPM for the selected best coolant oil of Therminol D-12. The 0.8 LPM VFR was determined to be optimal with the highest HTC of $2445.73 \text{ W/m}^2\cdot\text{K}$ and an acceptable pressure drop of 12,650 Pa, ensuring a balance between cooling performance and energy consumption. Finally, the cooling performance was evaluated at high charging/discharging C-rates from 1.5C to 3.0C for the proposed best coolant oil and VFR. The immersion cooling system with Therminol D-12 and a VFR of 0.8 LPM is an effective combination to achieve the desired performance of the battery module under extreme C-rate working conditions. The immersion cooling system with the proposed effective combination maintains the T_{\max} and ΔT at 38.6°C and 4.3°C under a charging rate of 3.0C and to 43.0°C and 5.5°C under a discharging rate of 3.0C.



Academic Editor: Hao Liu

Received: 25 December 2024

Revised: 24 January 2025

Accepted: 1 February 2025

Published: 3 February 2025

Citation: Tai, L.D.; Garud, K.S.; Lee, M.-Y. Experimental Study on Thermal Management of 5S7P Battery Module with Immersion Cooling Under High Charging/Discharging C-Rates. *Batteries* **2025**, *11*, 59. <https://doi.org/10.3390/batteries11020059>

Copyright: © 2025 by the authors. Licensee MDPI, Basel, Switzerland. This article is an open access article distributed under the terms and conditions of the Creative Commons Attribution (CC BY) license (<https://creativecommons.org/licenses/by/4.0/>).

1. Introduction

Growing global concerns about energy depletion and the urgent need to mitigate climate change have played a pivotal role in driving the rapid development and adoption of electric vehicles (EVs) [1]. Lithium-ion batteries (LIBs) are at the heart of this transformational change, with their exceptional benefits of high energy density, good performance, extended cycle life, no memory impact, and fast charging and discharging capabilities [2,3]. However, the performance of LIBs is significantly dependent on their temperature during charge/discharge cycles. To ensure optimal performance, LIBs must be maintained within a safe range of $25\text{--}40^\circ\text{C}$, and the ΔT within the battery module should not be greater than 5°C [4,5]. Operating at lower temperatures significantly reduces the battery capacity and charging efficiency. In contrast, higher temperatures cause faster cycle life loss and cause dangerous thermal problems [6–8]. Furthermore, the ΔT in the battery module also

plays a significant part in ensuring its performance and safety during operation. High temperature differences can lead to an uneven depth of discharge between battery cells, leading to a reduction in the battery module's overall performance. An uneven state of charge between battery cells leads to overcharge or over-discharge, resulting in a decrease in battery life [9,10]. According to studies, for every 5% increase in temperature difference, capacity can decrease by 2% [11]. In addition, the continuous development of electric vehicles with higher battery capacity and power has placed more stringent requirements on fast charging and discharging issues [12]. At higher charge and discharge rates, the heat generated by the battery also increases. Suppose the generated heat is not released in time. In that case, it may lead to heat accumulation, which increases internal chemical reactions, rapidly increases battery temperature, and could result in a thermal runaway and destruction of the battery pack [13–15]. Consequently, the investigation and advancement of battery thermal management systems (BTMS) are necessary to enhance the safety and optimal performance of LIBs [16,17].

Popular BTMSs are classified into air cooling, PCM cooling, and liquid cooling systems [18,19]. Because of its many benefits, including its straightforward design, low operating costs, and ease of maintenance, air cooling is frequently employed. However, because of its low specific heat capacity and poor thermal conductivity, air cooling is only appropriate for applications requiring little heat dissipation. Under harsh operating conditions, air cooling cannot meet the heat dissipation needs and is at risk of triggering dangerous thermal runaway in the battery module [12,20]. With the outstanding advantage of high latent heat, PCM cooling can maintain excellent temperature uniformity in the battery module through heat absorption and phase change mechanisms. This passive cooling method also offers advantages such as a compact structure and cost-effectiveness. However, the challenge facing PCM cooling systems is that they cannot effectively dissipate heat due to their low thermal conductivity, especially under harsh working conditions. Potential solutions to improve the thermal conductivity of PCMs include the incorporation of carbon, metal, or their oxide materials [21,22].

Direct and indirect liquid cooling are two categories of liquid cooling technologies [23]. With indirect liquid cooling, heat is exchanged with the battery module through cooling plates, cooling channels, and cooling jackets. In an indirect cooling system, the coolant is usually water or a water–ethylene glycol mixture. Compared with air-cooled systems, indirect liquid cooling has a higher specific heat capacity and thermal conductivity, which greatly improves the temperature uniformity and cooling performance of the battery module. However, the main obstacle of indirect cooling is the high thermal resistance between the battery module and the coolant, which significantly reduces the heat dissipation efficiency. In addition, the indirect cooling system also faces problems such as fluid leakage, a complex structure, and increased weight [24,25].

A direct liquid cooling system—also referred to as an immersion cooling system—improves cooling efficiency, temperature uniformity, and thermal resistance by submerging the battery cells in a dielectric coolant medium. This is because all of the battery cells' surfaces are directly exposed to the coolant. Especially under harsh operating conditions, immersion cooling systems can prevent and inhibit the propagation of thermal runaway phenomena, thus improving the reliability of LIB battery modules [26,27]. Furthermore, immersion cooling has the advantages of a simple structure, easy maintenance, and energy saving. Commonly used coolants in immersion cooling systems are mineral oil, silicone oil, ester, hydrocarbon oil, or fluorocarbon. Therefore, an immersion cooling system is considered a potential BTMS to provide efficient and safe thermal management for LIB battery packs with large capacities and those operating under harsh conditions [28,29].

For a six-cell battery module, Yanhui et al. suggested an immersion cooling technique that outperformed conventional air cooling by keeping the battery temperature under 40 °C and controlling ΔT below 3 °C during a 3.0C discharge [30]. The battery module transformer oil immersion cooling technique developed by Luyao et al. was examined. The findings indicated that at a 2.0C discharge rate, the battery module temperature was reduced by 26.3% compared to a natural air-cooling system [4]. Jiahao et al. assessed a mineral oil immersion cooling system's cooling effectiveness for a 16-cell lithium-ion battery module. According to the results, the immersion cooling system provided better cooling efficiency for the battery module than natural convection, reducing the maximum temperature rise for 1.0C, 2.0C, and 3.0C discharge rates by 40%, 45%, and 38%, respectively [31]. An immersion cooling structure was suggested by Choi et al. to enhance battery thermal management performance in harsh charging circumstances. This design maintains an ideal battery temperature at 3.0C charging while reducing the pressure drop by 45.4% and energy usage by 61.0% when compared to the baseline structure. Furthermore, in comparison to the traditional technique, immersion cooling lowers the T_{max} by 6.7 °C and the ΔT by 3.0 K [32]. Using synthetic ester oil, Hemavathi et al. assessed the single-phase forced immersion cooling (FFIC) method for controlling the temperature of 4S2P Li-ion battery packs, particularly in situations involving rapid discharge. The findings demonstrated that at a 3.0C discharge rate, FFIC produced an ideal temperature of 31.3 °C with outstanding ΔT . Furthermore, FFIC decreased the temperature increase by 35% when compared to static flow immersion cooling (SFIC) and 51% when compared to natural air convection [33]. The lithium-ion battery cooling technologies proposed by Satyanarayana et al. include mineral oil cooling (MOC), thermal oil cooling (TOC), and forced air cooling (FAC). When compared at a 3.0C discharge rate, the results show that FAC, TOC, and MOC significantly reduce the T_{max} of the battery module by 43.83%, 49.17%, and 51.54%, respectively, compared with the natural air-cooled system. This shows that low-cost liquid dielectric cooling is safe and suitable for high-capacity lithium-ion battery applications [34].

Although great progress has been made in the research of immersion cooling for the thermal management of lithium-ion batteries, there are still some gaps that need to be addressed. Most studies, such as those of Yanhui [30], Luyao [4], and Jiahao [31], have focused on battery modules with limited cell counts, failing to fully evaluate the cooling efficiency in larger modules with complex structures, such as the 5S7P module in the current study. In addition, a few studies, such as those of Choi [32] and Hemavathi [33], have tested different designs and coolant oils, but they have not fully considered the impact of harsh operating conditions such as a high charging/discharging C-rate, especially up to 3.0C as in this study. Moreover, the impact of coolant oil and VFR on the operation of battery modules with immersion cooling systems under high charging and discharging rates has not been thoroughly examined in prior research. This study addresses these gaps by experimentally evaluating the thermal management capabilities of an immersion cooling system for a larger 5S7P battery module under severe operating conditions at both high charging and discharging rates up to 3.0C. The novelty of the study lies in the identification and proposition of an optimal coolant oil and the optimal VFR for maintaining the desired cooling performance of the battery module at both high charging and discharging rates. The study not only provides comprehensive experimental data on the T_{max} and ΔT under these conditions but also evaluates the trade-off between cooling performance and energy consumption, which has not been fully investigated previously. This provides new insights and practical applications for high-energy density battery systems operating under extreme conditions.

2. Experiment Method

2.1. Battery Module and Coolant Oil

In the current investigation, a 21700-type battery cell (INR21700-48X-SDI-2) manufactured by Samsung SDI Co., Ltd. (Yongin-si, Republic of Korea) at the Cheonan Factory, Korea with a nominal capacity of 4.8 Ah was used for the evaluation with the immersion cooling method. The battery module consisted of 35 cells with a 5S7P configuration, of which five cells were linked together in series and seven cells were linked together in parallel as illustrated in Figure 1a. The 5S7P configuration was chosen in this study to balance the experimental feasibility and representativeness of real battery modules. The smaller size makes it easier to conduct experiments in the laboratory with available equipment, ensuring safety and good control of temperature, voltage, current, and pressure. Although the 5S7P configuration is smaller than modules commonly used in EVs, it still provides a suitable model for studying heat transfer and cooling performance, allowing the results to be applied to predict the behavior of larger modules. At the same time, using the 5S7P module helps to shrink the problem, saving costs and time while maintaining the important characteristics of real modules, thereby creating a foundation for future scalable studies and larger-scale applications. The characteristics of the cells and battery module taken into consideration in the investigation are shown in Table 1. The battery cells were arranged in an aligned configuration in an aluminum box with $163.0 \times 117.0 \times 90$ mm dimensions. The distance between the parallel and series connection configurations between the battery cells was 2 mm, and the distance between the battery cell and the aluminum box was 2 mm. With the benefits of low cost and great cooling efficiency, Therminol D-12, Pitherm 150B, and BOT 2100 were selected as coolant oils for battery modules with immersion cooling systems. Table 2 presents the properties of the coolant oils used in the present study. A 3-inlet and 3-outlet configuration of the coolant oil was established to ensure uniform distribution in the battery module. One crucial element that has a large impact on the battery module cooling effectiveness in immersion cooling systems is the coolant flow direction. The effect of flow direction on the thermal performance of LIB battery modules has been assessed in numerous studies. According to the study's findings, the bottom-to-top flow direction offers more cooling efficiency than the top-to-bottom flow path. A more even distribution of coolant is made possible by the bottom-to-top flow design, which raises the heat transfer coefficient, boosts cooling effectiveness, and keeps the battery module's temperature extremely consistent [32,35]. Therefore, the bottom-to-top coolant flow direction was adopted in the present experimental study. The height of the coolant inlet was set to 15 mm from the bottom of the aluminum box, and the height of the coolant outlet was set to 75 mm from the bottom of the aluminum box. As illustrated in Figure 1a, nine T-type thermocouples (T1–T9) were affixed to the surface of nine battery cells at various locations to gather temperature data during the experiment processes to assess the thermal performance of the battery module with an immersion cooling system under various circumstances. According to the studies, the temperature distribution of the cylindrical battery is considered to be uniform, with no significant difference between the top, middle, and bottom positions. The temperature at the middle location can be considered as the representative temperature of the entire battery surface [36–38]. Therefore, in this study, the thermocouples were attached to the middle position of the battery cells. Figure 1b displays the schematic diagram of the thermocouple mounting sites.

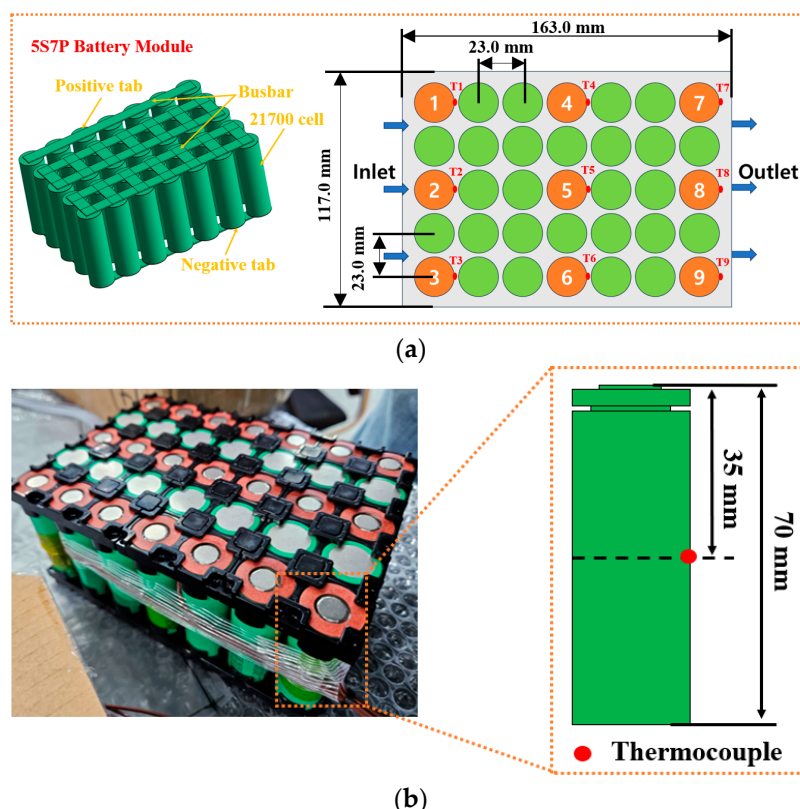


Figure 1. (a) Configuration of 5S7P battery module with immersion cooling; (b) Location of thermocouple installation in battery surface.

Table 1. Details of the battery module and cell used in the investigation.

Specifications	Value	Unit
Battery cell		
Nominal capacity	4.8	Ah
Nominal voltage	3.64	V
Maximum charge voltage	4.2	V
Discharge cut-off voltage	2.5	V
Diameter	21.15 ± 0.2	mm
Height	70.65 ± 0.15	mm
Weight	68.0 ± 1.5	g
Battery module		
Number of cells/modules	35	
Nominal battery module voltage	18.2	V
Maximum battery module voltage	21	V
Nominal battery module capacity	705.6	Wh

Table 2. Properties of coolant oils used in the present study.

Specifications	Therminol D-12	Pitherm 150B	BOT 2100
Density (kg/m^3)	758.5	785.99	797.0
Viscosity ($\text{kg}/(\text{m}\cdot\text{s})$)	0.001165	0.00632	0.00476
Specific heat capacity ($\text{J}/(\text{kg}\cdot\text{K})$)	2110	2188.3	2055
Thermal conductivity ($\text{W}/(\text{m}\cdot\text{K})$)	0.1092	0.1363	0.1377

2.2. Configuration for the Immersion Cooling 5S7P Battery Module Experiment

The immersion cooling experimental setup schematic diagram for the 5S7P battery module is displayed in Figure 2. A TOYOTECH TEX60-400 power supply (Aichi, Japan) was used to charge the battery module. The power supply had a maximum operating power of 24 kW, with operating voltage and current ranges of 60 V and 400 A, respectively. The battery module was discharged using a TOYOTECH TLF5000-A electric loader. The electric loader had a maximum operating power of 5 kW with operating voltage and current ranges of 150 V and 800 A, respectively. The coolant oil was cooled using a 5 kW JWT-30 chiller and heat exchanger, which also controlled and maintained the coolant oil's inlet temperature. To circulate the coolant oil in the immersion cooling system, a JIHPUMP peristaltic pump was utilized, which has an operating range of 0.4 mLPM to 2200 mLPM. The Data Logger GL820 was used to collect voltage, temperature, and pressure data of the battery module during the experiment. Nine T-type thermocouples were attached to the surface of different battery cells with an operating range of temperature from -220°C to 400°C . All experiments were carried out with an ambient temperature setting of 25°C in a constant temperature and humidity chamber.

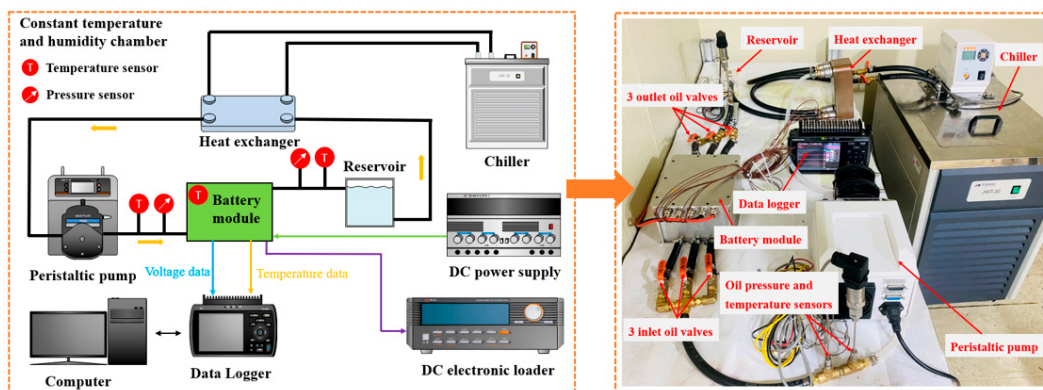


Figure 2. Diagrammatic representation of the experimental configuration for the immersion-cooled 5S7P battery module.

The constant current–constant voltage, or CC–CV, charging technique was used during the battery module charging process. The battery module's highest charging voltage during the CC charging procedure was 21 V. The charging process ended when the current reached the charge cut-off current status of the battery module at 0.84 A during the CV charging process. The battery module discharging process applied the CC (constant current) discharge method. The battery module fully charged at 21 V was discharged at different discharge rates. The discharge process ended when the voltage reached the discharge cut-off voltage of the battery module at 12.5 V. The charge/discharge rates conducted in the present study included 1.0C (33.6 A), 1.5C (50.4 A), 2.0C (67.2 A), 2.5C (84 A), and 3.0C (100.8 A).

To assess the efficiency of immersion cooling for battery modules, thermal and hydraulic performance criteria including T_{\max} , ΔT , HTC, and pressure drop (ΔP) were considered. Firstly, three types of coolant oils were experimentally investigated, namely, Therminol D-12, Pitherm 150B, and BOT 2100, with the coolant oil volume flow rate (VFR) at 0.6 LPM. Then, the optimal coolant oil was proposed for experimental investigation with different coolant oil VFR values from 0.4 LPM to 1 LPM. Finally, the optimal coolant oil with the optimal VFR was tested and evaluated for thermal management efficiency for battery modules at high charge/discharge rates up to 3.0C rates.

2.3. Data Reduction and Uncertainty Analysis

During the operating process, the battery's total heat generation (Q_{gen}) is computed by adding the heat from irreversible heating (Q_{irr}) and reversible heating (Q_{rev}), where irreversible heating is caused by Joule heating and reversible heating is caused by entropy generation [39].

$$Q_{gen} = Q_{irr} + Q_{rev} = I(U_{oc} - V_{bat}) - IT \frac{dU_{oc}}{dT} \quad (1)$$

Here, I stands in for the battery current as it is being charged or discharged. V_{bat} and U_{oc} represent battery and open-circuit voltages, respectively. T stands for battery temperature. The entropic coefficient is represented as $\frac{dU_{oc}}{dT}$.

The ΔT in the battery module during the experiment is calculated as follows [40]:

$$\Delta T = T_{max,battery} - T_{min,battery} \quad (2)$$

where $T_{max,battery}$ denotes the battery cells' maximum temperature and $T_{min,battery}$ denotes their minimum temperature.

The HTC is calculated as follows [40]:

$$h = \frac{Q_{conv,oil}}{A_{battery} (T_{mean,battery} - T_{mean,oil})} \quad (3)$$

The coolant oil mean temperature is calculated as follows [40]:

$$T_{mean,oil} = \frac{T_{inlet,oil} + T_{outlet,oil}}{2} \quad (4)$$

The heat generated from the battery absorbed by the coolant oil is calculated as follows [40]:

$$Q_{conv,oil} = \dot{m}_{oil} C_{p,oil} (T_{outlet,oil} - T_{inlet,oil}) \quad (5)$$

The following formula is used to determine the pressure drop of coolant oil [41]:

$$\Delta P_{oil} = P_{inlet,oil} - P_{outlet,oil} \quad (6)$$

where $A_{battery}$ indicates the area of the battery surface; $T_{mean,battery}$ indicates the mean temperature of the battery; $T_{mean,oil}$ indicates the mean temperature of coolant oil; $T_{outlet,oil}$ and $T_{inlet,oil}$ indicate outlet and inlet temperatures of coolant oil; \dot{m}_{oil} , $C_{p,oil}$ indicate the mass flow rate and heat capacity of coolant oil; and $P_{inlet,oil}$ and $P_{outlet,oil}$ indicate the inlet and outlet pressure of coolant oil.

Factors such as measurement error, deviation in probe position, environmental conditions, and inadequate calibration can lead to inaccuracies in the measured experimental parameters [38]. To ensure the accuracy and reliability of the data, the study performed an uncertainty analysis based on the parameters provided in the manufacturer's datasheet. Specifically, the accuracy of the DC electronic loader, T-type thermocouple, Pt-100 temperature sensor, peristaltic pump, and data logger were $\pm 0.1\%$, $\pm 0.5\%$, $\pm 0.25\%$, $\pm 0.2\%$, and $\pm 0.1\%$, respectively.

Uncertainty analysis was performed based on the experimental equipment used and factors such as probe position, calibration, and measurement error. The uncertainties of the main experimental parameters are calculated through Equation (7) [40]:

$$U_R = \left[\left(\frac{\partial R}{\partial X_1} U_1 \right)^2 + \left(\frac{\partial R}{\partial X_2} U_2 \right)^2 + \left(\frac{\partial R}{\partial X_3} U_3 \right)^2 + \cdots + \left(\frac{\partial R}{\partial X_n} U_n \right)^2 \right]^{\frac{1}{2}} \quad (7)$$

where R is the dependent experimental parameter, U_R is the uncertainty of this parameter, and $X_1, X_2, X_3, \dots, X_n$ are the independent experimental parameters, with $U_1, U_2, U_3, \dots, U_n$ being the corresponding uncertainties.

The results showed that the uncertainties of the evaluated parameters were as follows: temperature $\pm 1.31\%$, pressure $\pm 1.14\%$, and heat transfer coefficient $\pm 4.07\%$, respectively. All devices and sensors in this study were carefully calibrated before conducting the experiment to minimize measurement errors.

3. Results and Discussion

This part assessed the 5S7P battery module's thermal and hydraulic performance using the T_{max} , ΔT , HTC, and ΔP criteria under various immersion cooling system operating circumstances. First, the thermal management efficiency of immersion cooling was evaluated with different coolant oils, including Therminol D-12, Pitherm 150B, and BOT 2100, to propose the optimal coolant oil in Section 3.1. In Section 3.2, with the proposed optimal coolant oil, the impact of various VFR values on the cooling efficiency of immersion cooling was considered from 0.4 LPM to 1 LPM. Finally, the cooling efficiency for the battery module using immersion cooling based on the optimized coolant oil and VFR was considered and evaluated at high charge/discharge rates up to 3.0C in Section 3.3.

3.1. Different Coolant Oils

In this section, the impact of different types of coolant oils on the cooling efficiency of immersion cooling for 5S7P battery modules was evaluated including Therminol D-12, Pitherm 150B, and BOT 2100. The parameters evaluated included T_{max} , ΔT , HTC, and ΔP . Experiments with different coolant oils were conducted under the same conditions of a 0.6 LPM volume flow rate, a constant coolant oil inlet temperature, and ambient temperature maintained at 25 °C.

The temperature distribution in the immersion cooling battery module with different types of coolant oils is shown in Figure 3. The findings indicate that the temperature in the battery module tends to increase gradually along the coolant oil flow direction. Specifically, the temperature of the battery cells near the coolant oil inlet (T1–T3) is the lowest due to direct contact with the coolant oil at low temperatures. On the other hand, the battery cells in the middle and end regions of the module (T4–T6 and T7–T9) have higher temperatures, with the highest values at the locations near the coolant oil outlet (T7–T9). This difference is explained by the decreasing heat dissipation efficiency along the flow direction. In the area near the coolant oil inlet, the high-temperature gradient between the coolant oil and the battery cells enhances the heat transfer process, resulting in a lower temperature. However, in the area near the outlet, the coolant oil has exchanged heat with the previous battery cells, causing its temperature to increase. This reduces the temperature gradient between the coolant oil and the battery cells, resulting in lower heat dissipation efficiency and higher temperatures. Notably, the temperatures at locations T5 and T8 were found to be the highest in the battery module. This is mainly because these locations are located in the center and near the outlet of the coolant flow, where the most heat accumulates during operation. This explains the appearance of hot spots in the module, especially in the central and near-end regions of the flow.

The variation in the T_{max} and ΔT of the immersion cooling battery module with different types of coolant oils is illustrated in Figure 4. Due to their superior specific heat capacity and thermal conductivity, the selected coolant oils demonstrated outstanding cooling performance, effectively maintaining the T_{max} and ΔT of the battery module within an optimal range at a discharge rate of 1.0C. Among the oils, Therminol D-12 exhibited the most effective thermal management, achieving the lowest T_{max} and ΔT of 31.1 °C and

$2.1\text{ }^{\circ}\text{C}$, respectively, representing reductions of 8.52% and 52.2% compared to BOT 2100. In contrast, the other two coolant oils, Pitherm 150B and BOT 2100, resulted in higher T_{\max} values of $33.7\text{ }^{\circ}\text{C}$ and $34.0\text{ }^{\circ}\text{C}$ and higher ΔT values of $4.0\text{ }^{\circ}\text{C}$ and $4.4\text{ }^{\circ}\text{C}$, respectively. These differences can be attributed to the lower viscosity and density of Therminol D-12, which facilitates a more uniform distribution of the coolant oil and allows it to flow more efficiently within the battery module. Consequently, this enhances heat dissipation and accelerates heat removal from the battery module, resulting in a significant reduction in temperature compared to the other two coolant oils.

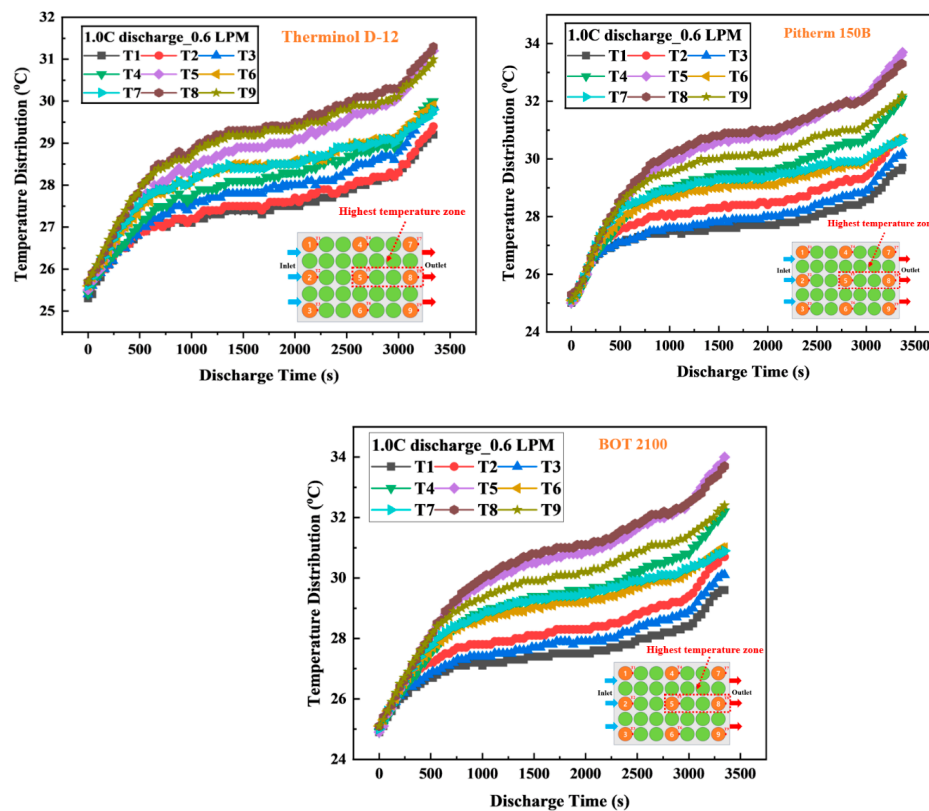


Figure 3. Temperature distribution in immersion cooling battery module with different types of coolant oils.

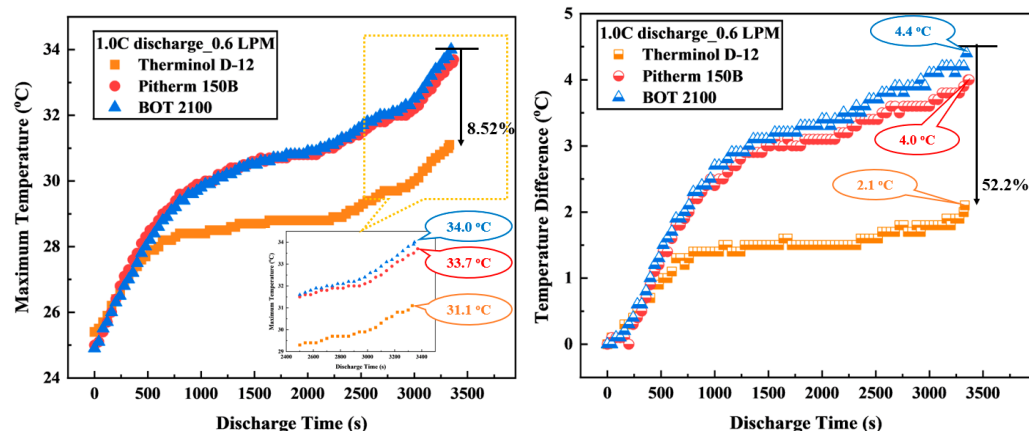


Figure 4. Variation in T_{\max} and ΔT of immersion cooling battery module with different types of coolant oils.

Figure 5 displays the change in the HTC over time for various coolant oil types. The HTC showed a clear difference between the oils based on their physical and thermal properties. Therminol D-12 achieved the highest heat transfer efficiency, with an HTC

of $2171.93 \text{ W/m}^2\cdot\text{K}$. This can be explained by the superior properties of Therminol D-12, including high specific heat capacity and thermal conductivity, along with low viscosity and density, which optimize the heat transfer process. In contrast, although Pitherm 150B and BOT 2100 have a higher specific heat capacity and thermal conductivity than Therminol D-12, they are limited by their higher density and viscosity. These factors increase the resistance to heat transfer, resulting in lower HTC values of $1462.58 \text{ W/m}^2\cdot\text{K}$ and $1183.52 \text{ W/m}^2\cdot\text{K}$. This result emphasizes the importance of balancing the fluid's thermophysical and dynamic properties in improving the system's cooling performance.

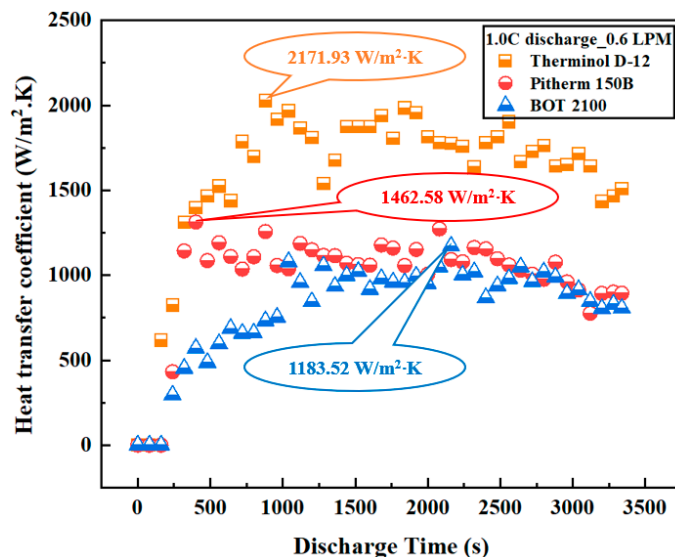


Figure 5. Variation in HTC with time for different types of coolant oils.

Pressure drop is a crucial factor for evaluating the energy efficiency of cooling systems. Cooling systems with lower pressure drops consume less energy, whereas higher pressure drops result in greater energy consumption. The variation in the pressure drops of the immersion cooling system with different coolant oils is presented in Figure 6. Research findings indicated that Therminol D-12 achieved the lowest pressure drop, at 8880 Pa, while Pitherm 150B and BOT 2100 exhibited higher pressure drops of 9840 Pa and 10,310 Pa, respectively. This result is attributable to the lower density and viscosity of Therminol D-12, which improved flow efficiency within the battery module and reduced the pressure differential compared to the other coolants. These findings highlight the significant influence of the thermophysical properties of coolant oils on cooling performance and energy consumption in cooling systems, particularly in immersion cooling methods.

Based on the research results, Therminol D-12 was identified as the optimal coolant oil for use in immersion cooling systems for 5S7P lithium-ion battery modules due to its outstanding thermophysical properties and superior cooling performance, proven through numerous experiments. Therminol D-12 possesses superior thermophysical properties, including low viscosity ($0.001165 \text{ kg/m}\cdot\text{s}$ at 25°C), high specific heat capacity ($2110 \text{ J/kg}\cdot\text{K}$ at 25°C), and good thermal conductivity ($0.1092 \text{ W/m}\cdot\text{K}$ at 25°C). These properties play an important role in improving heat transfer efficiency. Low viscosity allows the oil to flow easily through the system, minimizing pressure drops and pumping energy consumption. The high specific heat capacity enables Therminol D-12 to absorb and store a larger amount of heat, while the high thermal conductivity ensures efficient heat transfer between the cell surface and the coolant oil. In the experiments, Therminol D-12 achieved the highest heat transfer coefficient ($2171.93 \text{ W/m}^2\cdot\text{K}$), the lowest T_{\max} (31.1°C), and the smallest ΔT between cells in the battery module (2.1°C), demonstrating superior thermal control performance. At the same time, the oil achieved the lowest pressure drop (8880 Pa),

which reduced energy consumption during operation and improved the overall energy efficiency of the cooling system. These factors were quantitatively correlated with the cooling performance of Therminol D-12, demonstrating the optimal balance between heat transfer efficiency and energy consumption. These results not only ensure efficient cooling but also reduce energy consumption, making Therminol D-12 a superior coolant choice for further experiments with higher charge/discharge rates. In addition, the study also shows that optimizing the thermophysical properties of the coolant can play an important role in improving the cooling performance of immersion systems in future applications.

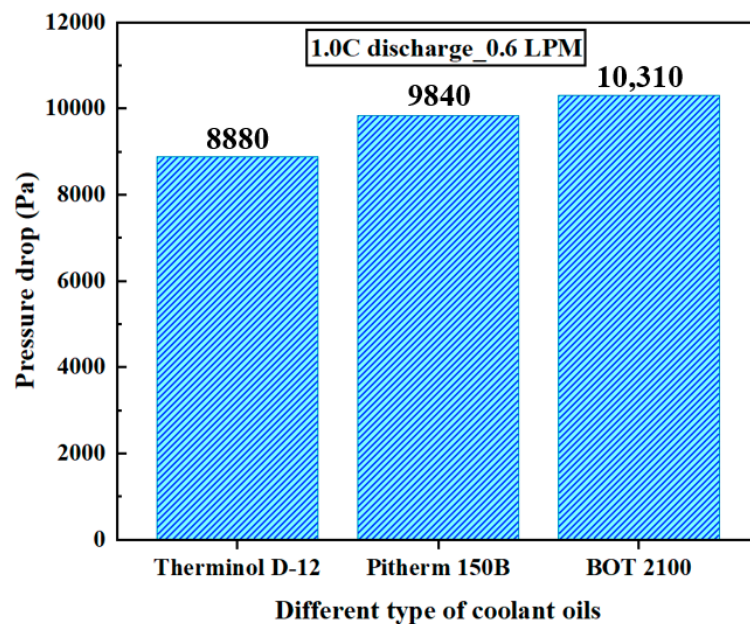


Figure 6. Pressure drop variation in the immersion cooling battery module with different types of coolant oils.

3.2. Volume Flow Rates

In this section, the influence of the optimal coolant oil proposed in Section 3.1 with different VFR values on the cooling effectiveness of immersion cooling was analyzed. Specifically, Therminol D-12 with different VFR values, ranging from 0.4 LPM to 1.0 LPM, was studied under the condition of discharge rate of 1.0C. The coolant oil and ambient temperature were maintained at 25 °C.

The variation in T_{max} and ΔT at different VFRs is demonstrated in Figure 7. The results show that Therminol D-12 achieved superior cooling performance, maintaining the T_{max} and ΔT in the battery module at optimal levels at all VFRs from 0.4 LPM to 1.0 LPM. Specifically, larger flow rates resulted in higher cooling efficiency, with the T_{max} and ΔT ranging from 31.1 °C to 31.2 °C and from 1.9 °C to 2.1 °C as the VFR increased from 0.6 LPM to 1.0 LPM. In contrast, at lower VFRs, the cooling efficiency decreased significantly, with the T_{max} and ΔT being 31.4 °C and 2.4 °C, respectively, at 0.4 LPM.

The explanation for this phenomenon is that the larger VFRs increase the heat exchange rate of the battery cells with the coolant oil, which helps to remove heat from the battery more quickly and efficiently, thereby improving the heat dissipation capacity and significantly reducing the battery temperature. However, increasing the coolant oil VFR to high values does not mean that the cooling efficiency will continue to improve, as this efficiency tends to be saturated when reaching a certain VFR. The research results show that when the coolant oil VFR increases from 0.8 LPM to 1.0 LPM, the difference in T_{max} and ΔT is only 0.1 °C, which is negligible. In addition, increasing the coolant oil VFR also results in a significant increase in the pressure drop, thereby increasing energy

consumption. Consequently, determining and evaluating the appropriate coolant oil VFR is essential to ensure a balance between cooling effectiveness and energy consumption in the immersion cooling system.

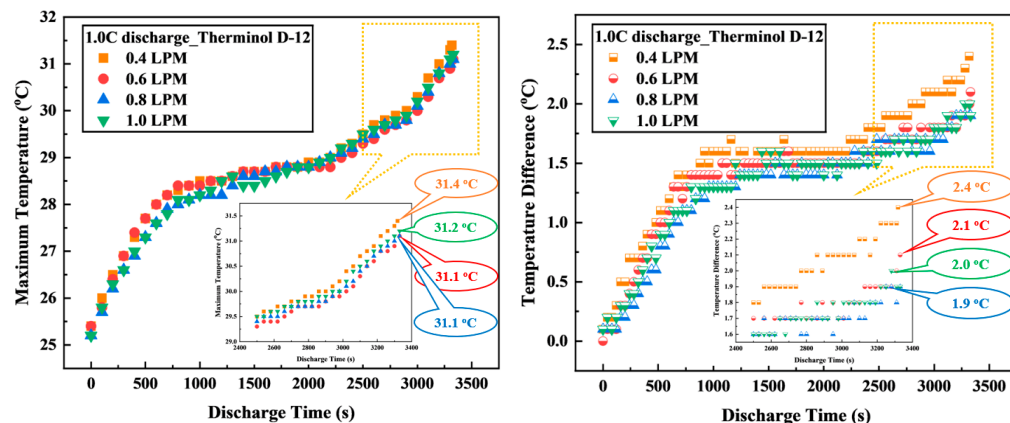


Figure 7. Variation in the T_{\max} and ΔT of the immersion cooling battery module with different volume flow rates.

Figure 8 shows the variation in the HTC of Therminol D-12 with different VFRs at a discharge rate of 1.0C, demonstrating the significant impact of VFR on cooling performance. At a VFR of 0.4 LPM, the HTC reached $1370.25 \text{ W/m}^2\cdot\text{K}$, the lowest among the flow rates, due to the slow flow rate resulting in limited heat exchange capacity. When the VFR was increased to 0.6 LPM and 0.8 LPM, the HTC increased significantly to $2171.93 \text{ W/m}^2\cdot\text{K}$ and $2445.73 \text{ W/m}^2\cdot\text{K}$ due to the improvement in convection capacity and heat transfer efficiency. However, at 1.0 LPM, the HTC decreased slightly to $2354.39 \text{ W/m}^2\cdot\text{K}$, possibly due to the occurrence of heat transfer efficiency degradation when the coolant flow rate was too high, causing flow disturbance and reducing the heat contact time. This result emphasizes that, although increasing the coolant oil VFR improves the cooling efficiency, it is necessary to optimize the VFR to achieve a balance between heat transfer efficiency and energy efficiency, with the optimal VFR in this case being approximately 0.8 LPM.

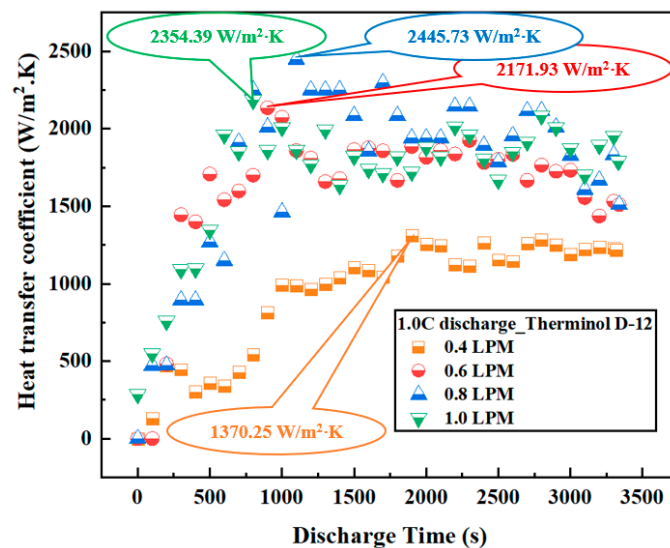


Figure 8. Variation in HTC with different volume flow rates.

The results in Figure 8 show that as the coolant VFR increases, the HTC in the battery module improves significantly. However, this improvement is not clearly shown in Figure 7 when considering the T_{\max} or ΔT . Specifically, when increasing the VFR from 0.4 LPM to

0.8 LPM, the T_{max} decreases from 31.4 °C to 31.1 °C, while the ΔT decreases from 2.4 °C to 1.9 °C. The main reason is that the battery module is operated at a discharge rate of 1.0C in this case. This normal discharge rate causes a relatively low amount of heat generation during the operation of the battery module. With this low amount of heat generated, when increasing the VFR, the heat is removed faster and the temperature distribution is improved. Still, these changes are not large enough to cause a significant difference in the T_{max} or ΔT . In addition, the immersion cooling system is highly efficient due to the coolant being in direct contact with the battery cell surface, which helps to maintain a uniform temperature distribution even when the VFR changes. Therefore, at a discharge rate of 1.0C, the difference in temperature distribution between VFR levels within the study range is negligible, as shown in Figure 7.

The variation in pressure drops with different VFRs of Therminol D-12 at a discharge rate of 1.0C in Figure 9 demonstrates the clear impact of the flow rate on the energy efficiency of the system. At a VFR of 0.4 LPM, the pressure drop reached its lowest level, only 8060 Pa, due to the slow flow, minimizing resistance in the system. As the VFR increased to 0.6 and 0.8 LPM, the pressure drop increased to 8880 Pa and 12,650 Pa, respectively, due to the increasing resistance from the faster flow. Notably, at the highest VFR of 1.0 LPM, the pressure drop increased sharply to 17,700 Pa, reflecting the influence of oil viscosity and density on effective flow resistance. This result highlights that, although higher VFRs can enhance heat transfer efficiency, they also lead to higher energy consumption due to increased pressure drops. Therefore, VFR optimization is essential to achieve a trade-off between cooling efficiency and energy consumption, with a medium VFR such as 0.6–0.8 LPM being the optimal choice in this case.

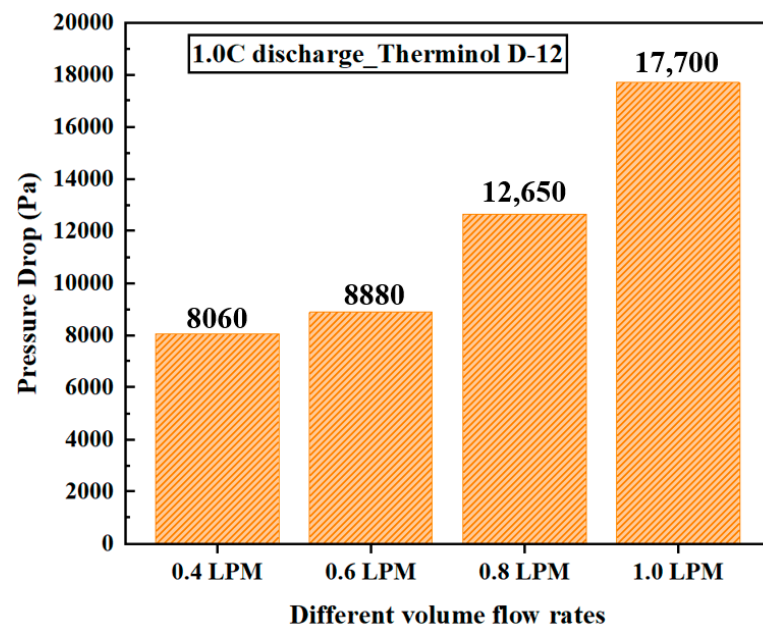


Figure 9. Pressure drop variation in the immersion cooling battery module with different volume flow rates.

The study results showed a significant impact of different coolant VFRs on the thermal performance of the battery module with immersion cooling. When increasing the VFR from 0.4 LPM to 0.8 LPM, the heat transfer performance of the system was significantly improved. Specifically, HTC increased from 1370.25 W/m²·K at 0.4 LPM to a maximum of 2445.73 W/m²·K at 0.8 LPM, with an increase of 12.60% compared to 0.6 LPM (2171.93 W/m²·K). At the same time, the T_{max} in the battery module was maintained at a minimum of 31.1 °C, while the ΔT between cells decreased from 2.1 °C at 0.6 LPM to 1.9 °C

at 0.8 LPM. These results demonstrate that 0.8 LPM provides superior thermal control performance in maintaining uniform temperature distribution in the battery module. Although the ΔT between 0.6 LPM and 0.8 LPM is not significant at a discharge rate of 1.0C due to the relatively low heat generated at normal discharge rates, at higher charge/discharge rates, with larger heat generated, higher coolant flow rates (i.e., 0.8 LPM) are expected to demonstrate superior cooling performance. This is because the higher HTC at 0.8 LPM improves the heat exchange efficiency and maintains a better temperature distribution. In addition, when the VFR increases to 1.0 LPM, although the HTC remains high (2354.39 W/m²·K), the cooling performance does not improve significantly compared to 0.8 LPM, while the pressure drop increases sharply to 17,700 Pa, resulting in higher energy consumption and lower overall efficiency. At 0.8 LPM, the pressure drop only reaches 12,650 Pa, which is within the acceptable range, ensuring a balance between cooling performance and energy consumption. Therefore, 0.8 LPM is determined to be the optimal VFR for the immersion cooling system in this study and is proposed for application in subsequent experiments at higher charge/discharge rates to further demonstrate the efficiency of the system.

3.3. Effectiveness of Thermal Management Under High C-Rate Charging Conditions

This section focuses on evaluating the thermal performance of the immersion cooling battery module at high charging rates ranging from 1.5C to 3.0C. To control the T_{max} and ΔT of the battery module within the optimal range, the experiments were conducted using Therminol D-12 coolant oil, which was identified as optimal in the previous sections due to its superior cooling performance, along with a VFR of 0.8 LPM. The choice of high charging rates helps to evaluate the system's ability to manage heat under harsh operating conditions and confirms the effectiveness and practical applicability of the immersion cooling system.

The results in Figure 10 show that the immersion cooling system with Therminol D-12 oil and an optimized VFR of 0.8 LPM maintained the T_{max} of the battery module within the control range even at high charging rates. Specifically, the T_{max} values measured were 32.7 °C, 35.1 °C, 37.0 °C, and 38.6 °C at charging rates of 1.5C, 2.0C, 2.5C, and 3.0C, respectively. These values are all below the optimal temperature threshold for lithium-ion batteries, ensuring thermal safety and minimizing the risk of performance degradation or battery failure. The increase in temperature with the charging rate is inevitable due to the larger current, but the immersion cooling system demonstrated effective thermal control, ensuring that the maximum temperature did not exceed the dangerous threshold. This confirms the important role of the immersion cooling system in ensuring stable battery operation even under harsh charging conditions.

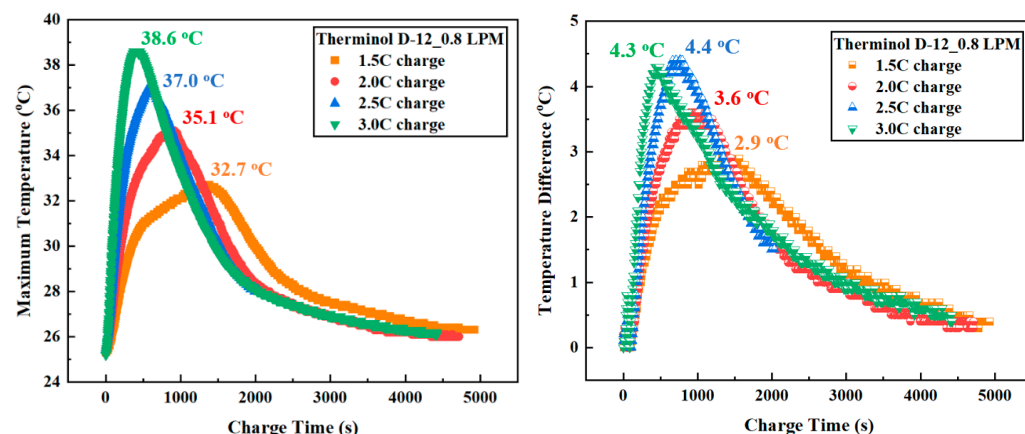


Figure 10. Variation in the T_{max} and ΔT of the immersion cooling battery module under different high C-rate charging conditions.

In addition to T_{max} control, the immersion cooling system also maintains the ΔT in the battery module at an optimal level, ensuring temperature uniformity between battery cells. The recorded ΔT values were 2.9 °C, 3.6 °C, 4.4 °C, and 4.3 °C at charging rates of 1.5C, 2.0C, 2.5C, and 3.0C, respectively. At the highest charging rate (3.0C), the ΔT decreased slightly compared to 2.5C, demonstrating the ability of the immersion cooling system to distribute heat evenly even under high thermal load conditions. This ability to control the ΔT not only increases battery life and performance but also minimizes the risk of thermal imbalance between cells. This once again confirms the outstanding performance of the immersion cooling system in this study, meeting the stringent requirements for thermal management at high charging rates.

3.4. Effectiveness of Thermal Management Under High C-Rate Discharging Conditions

This section focuses on evaluating the effectiveness of an immersion cooling system for 5S7P battery modules operating at high discharge rates from 1.5C to 3.0C. The experiments were conducted with Therminol D-12 coolant oil—which has been identified as optimal due to its superior cooling performance—along with a VFR of 0.8 LPM, as proposed in previous research sections. The objective is to control the T_{max} and ΔT parameters of the battery module within the ideal range to ensure the efficiency and safety of the battery even when operating at high discharge conditions, which often generate large amounts of heat and pose a risk of overheating.

The Therminol D-12 oil immersion cooling system and 0.8 LPM VFR demonstrated the ability to maintain the T_{max} of the battery module inside the near-optimal range at high discharge rates, as shown in Figure 11. Specifically, the T_{max} reached 33.8 °C, 36.8 °C, 39.8 °C, and 43.0 °C at discharge rates of 1.5C, 2.0C, 2.5C, and 3.0C, respectively. While the T_{max} from 1.5C to 2.5C was within the ideal range (below 40 °C), the temperature at 3.0C (43.0 °C) was slightly above this range. However, this temperature level was still acceptable and did not pose a serious risk of overheating. This result confirms the effectiveness of the immersion cooling system in temperature control, helping to maintain stability and safety for the battery even when operating at high discharge rates where rapid temperature increases are inevitable.

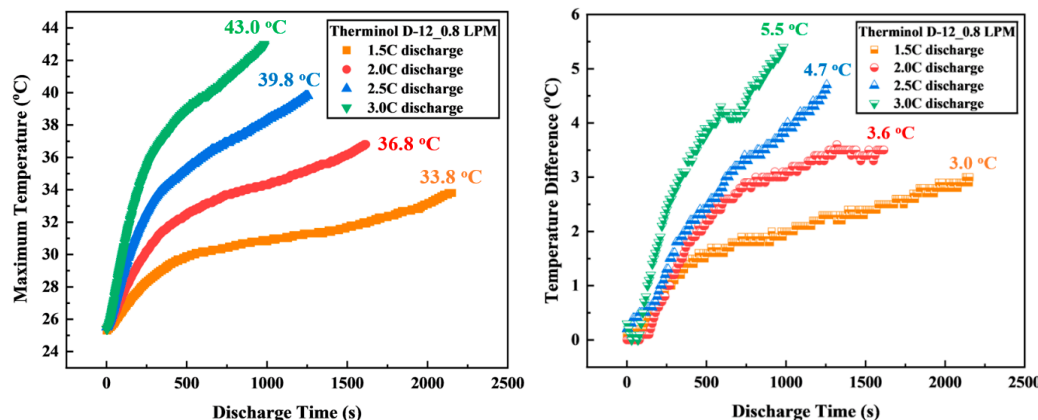


Figure 11. Variation in the T_{max} and ΔT of the immersion cooling battery module under different high C-rate discharging conditions.

In addition to T_{max} control, the immersion cooling system also ensures temperature uniformity within the battery module, as demonstrated by a well-controlled ΔT . The ΔT values were 3.0 °C, 3.6 °C, 4.7 °C, and 5.5 °C at 1.5C, 2.0C, 2.5C, and 3.0C discharge rates, respectively. The ΔT from 1.5C to 2.5C is within the ideal range (below 5 °C), which helps to maintain uniformity between the battery cells and minimize the possibility of thermal imbalance. Although the ΔT at 3.0C (5.5 °C) slightly exceeds the optimum threshold, it is

still within the acceptable range. The ability to effectively control the temperature difference even at high discharge rates emphasizes the superiority of the immersion cooling system in ensuring thermal safety and increasing the life and performance of lithium-ion batteries when operating under harsh conditions.

4. Conclusions

This study focuses on the performance evaluation of an immersion cooling system for a 5S7P battery module under various operating conditions, including different coolant oil types, different volume flow rates, and high charging/discharging rates. The following highlights the study's primary findings:

- (a) Therminol D-12 maintains the T_{max} of the battery module at 31.1 °C, which increased to 33.7 °C and 34.0 °C in the cases of Pitherm 150B and BOT 2100. Therminol D-12 achieved the highest HTC of 2171.93 W/m²·K and the lowest pressure drop of 8880 Pa compared to other coolant oils. Hence, Therminol D-12 was determined to be the best coolant oil for the immersion cooling system.
- (b) Therminol D-12 at a 0.8 LPM volume flow rate achieved an HTC of 2445.73 W/m²·K and maintained the T_{max} and ΔT of the battery module within the optimal range. The 0.4 LPM flow rate resulted in low cooling performance, while the 1.0 LPM flow rate resulted in a high pressure drop. Therefore, the 0.8 LPM flow rate was proposed as the optimal volume flow rate to ensure a balance between cooling performance and energy consumption.
- (c) The immersion cooling system with Therminol D-12 could maintain T_{max} values of 32.7 °C, 35.1 °C, 37.0 °C, and 38.6 °C and ΔT values of 2.9 °C, 3.6 °C, 4.4 °C, and 4.3 °C for battery module charging under 1.5C, 2.0C, 2.5C, and 3.0C rates, respectively. These values are all below the optimal temperature threshold, emphasizing the cooling system's effectiveness in thermal management and ensuring the thermal safety of the battery module even at high charging rates.
- (d) The T_{max} values of 33.8 °C, 36.8 °C, 39.8 °C, and 43.0 °C and ΔT values of 3.0 °C, 3.6 °C, 4.7 °C, and 5.5 °C were observed for the battery module under discharging rates of 1.5C, 2.0C, 2.5C, and 3.0C, respectively. Although the T_{max} and ΔT at the 3.0C discharge rate were slightly above the optimal threshold (40 °C and 5 °C), they were still within acceptable ranges, indicating that the immersion cooling system can operate effectively even under high thermal loads.

This study demonstrated the superior performance of the immersion cooling system in controlling the T_{max} and ΔT of the battery module within a safe range even under extreme operating conditions such as high charge/discharge values. With Therminol D-12 coolant oil and a VFR of 0.8 LPM, the cooling system ensures optimal cooling performance, helping to maintain the thermal safety and long-term performance of the LIBs. In the future, the study can be extended to test the cooling performance of the system with different battery module designs and more optimized immersion cooling configurations, as well as the applicability under real-world environmental conditions.

Author Contributions: Conceptualization, L.D.T. and M.-Y.L.; methodology, L.D.T., K.S.G. and M.-Y.L.; formal analysis, L.D.T. and M.-Y.L.; investigation, L.D.T., K.S.G. and M.-Y.L.; resources, L.D.T., K.S.G. and M.-Y.L.; data curation, L.D.T., K.S.G. and M.-Y.L.; writing—original draft preparation, L.D.T. and K.S.G.; writing—review and editing, L.D.T., K.S.G. and M.-Y.L.; visualization, L.D.T. and K.S.G.; supervision, M.-Y.L.; project administration, M.-Y.L.; funding acquisition, M.-Y.L. All authors have read and agreed to the published version of the manuscript.

Funding: This work was supported by the Dong-A University research fund.

Data Availability Statement: The data presented in this study are available upon request to the corresponding author. The data are not publicly available due to privacy.

Conflicts of Interest: The authors declare no conflicts of interest.

References

1. Jan, W.; Khan, A.D.; Iftikhar, F.J.; Ali, G. Recent advancements and challenges in deploying lithium sulfur batteries as economical energy storage devices. *J. Energy Storage* **2023**, *72*, 108559. [[CrossRef](#)]
2. He, Q.; Li, X.; Shan, W.; Zhang, W.; Wang, J.; Wang, Z.; Zheng, L. Numerical and experimental investigations on heat transfer characteristics and influencing factors of immersion cooling system for high-capacity prismatic lithium-ion battery. *J. Energy Storage* **2024**, *104*, 114518. [[CrossRef](#)]
3. Han, J.-W.; Hwang, S.-G.; Garud, K.S.; Lee, M.-S.; Lee, M.-Y. Numerical Study on Oil Cooling Performance of the Cylindrical Lithium-Ion Battery Pack with Flow Arrangement. *J. Korea Acad. Ind. Coop. Soc.* **2022**, *23*, 19–25. [[CrossRef](#)]
4. Zhao, L.; Tong, J.; Zheng, M.; Chen, M.; Li, W. Experimental study on the thermal management performance of immersion cooling for 18650 lithium-ion battery module. *Process Saf. Environ. Prot.* **2024**, *192*, 634–642. [[CrossRef](#)]
5. He, Z.; Chen, Y.; He, D. Effect of turning conditions on the indirect liquid-cooled battery thermal management in the electric vehicle. *Appl. Therm. Eng.* **2024**, *257*, 124418. [[CrossRef](#)]
6. Gao, Q.; Lu, Y.; Liu, X.; Chen, Y. A novel pulse liquid immersion cooling strategy for Lithium-ion battery pack. *Energy* **2024**, *310*, 133266. [[CrossRef](#)]
7. Donmez, M.; Karamangil, M.I. Artificial neural networks-based multi-objective optimization of immersion cooling battery thermal management system using Hammersley sampling method. *Case Stud. Therm. Eng.* **2024**, *64*, 105509. [[CrossRef](#)]
8. Lim, G.-P.; Kim, M.-S. Demonstration study about fire detecting, protecting and extinguishing method of ESS lithium-ion battery. *J. Korea Acad. Ind. Coop. Soc.* **2023**, *24*, 556–563.
9. Bao, R.; Wang, Z.; Yang, H.; Zhang, B.; Gao, Q.; Chen, S. Comparison analysis of thermal behavior of Lithium-ion batteries based on a novel multi-modal composite immersion liquid cooling system coupled with fin/micro-heat pipe array. *J. Energy Storage* **2024**, *104*, 114379. [[CrossRef](#)]
10. Choi, H.; Jun, Y.; Chun, H.; Lee, H. Comprehensive feasibility study on metal foam use in single-phase immersion cooling for battery thermal management system. *Appl. Energy* **2024**, *375*, 124083. [[CrossRef](#)]
11. Shi, Q.; Liu, Q.; Zhang, B.; Yao, X.; Zhu, X.; Ju, X.; Xu, C. Multi-objective optimization of an immersion cooling battery module with manifold jet impingement: Based on precision model for high-capacity batteries. *Int. Commun. Heat Mass Transf.* **2025**, *161*, 108448. [[CrossRef](#)]
12. Suresh, C.; Awasthi, A.; Kumar, B.; Im, S.; Jeon, Y. Advances in battery thermal management for electric vehicles: A comprehensive review of hybrid PCM-metal foam and immersion cooling technologies. *Renew. Sustain. Energy Rev.* **2025**, *208*, 115021. [[CrossRef](#)]
13. Hussain, M.; Khan, M.K.; Pathak, M. Thermal management of high-energy lithium titanate oxide batteries using an effective channeled dielectric fluid immersion cooling system. *Energy Convers. Manag.* **2024**, *313*, 118644. [[CrossRef](#)]
14. Li, Y.; Bai, M.; Zhou, Z.; Wu, W.; Lv, J.; Gao, L.; Huang, H.; Li, Y.; Song, Y. Experimental studies of reciprocating liquid immersion cooling for 18650 lithium-ion battery under fast charging conditions. *J. Energy Storage* **2023**, *64*, 107177. [[CrossRef](#)]
15. Choi, H.-S.; Hwang, S.-Y.; Kim, N.-H.; Kim, H.-J.; Kim, J.-M.; Rho, D.-S. A Study on Fire Detection Algorithm in ESS by Considering Fire Mechanism for Li-ion Battery. *J. Korea Acad. Ind. Coop. Soc.* **2024**, *25*, 538–547.
16. Li, W.; Wang, Y.; He, B.; Guo, J.; Ju, G.; Yu, Z.; Chen, Z.; Jiang, F. Influence of structural parameters on immersion cooling performance of a 1P52S 280 Ah prismatic LiFePO₄ battery pack. *Appl. Therm. Eng.* **2025**, *261*, 125185. [[CrossRef](#)]
17. Liu, X.; Zhou, Z.; Wu, W.; Wei, L.; Hu, C.; Li, Y.; Huang, H.; Li, Y.; Song, Y. Numerical simulation for comparison of cold plate cooling and HFE-7000 immersion cooling in lithium-ion battery thermal management. *J. Energy Storage* **2024**, *101*, 113938. [[CrossRef](#)]
18. Shi, H.; Zeng, Z.; Kong, B.; Yuan, N. Enhancing high-density battery performance through innovative single-phase spray technology in immersion cooling systems. *J. Power Sources* **2025**, *626*, 235770. [[CrossRef](#)]
19. Shi, Q.; Liu, Q.; Liu, Y.; Yao, X.; Zhu, X.; Ju, X.; Xu, C. Optimization of an immersion cooling 46.5 kW/46.5 kWh battery module using flow resistance network shortcut method. *J. Energy Storage* **2024**, *103*, 114383. [[CrossRef](#)]
20. Ye, Y.; Mao, Y.; Zhao, L.; Chen, Y.; Chen, M. Experimental investigation of thermal runaway behavior and propagation inhibition of lithium-ion battery by immersion cooling. *Appl. Therm. Eng.* **2024**, *256*, 124093. [[CrossRef](#)]
21. Huang, H.; Li, W.; Xiong, S.; Luo, Z.; Ahmed, M. Single-phase static immersion-cooled battery thermal management system with finned heat pipes. *Appl. Therm. Eng.* **2024**, *254*, 123931. [[CrossRef](#)]
22. Ahmad, S.; Liu, Y.; Khan, S.A.; Shah, S.W.A.; Huang, X. Modeling liquid immersion-cooling battery thermal management system and optimization via machine learning. *Int. Commun. Heat Mass Transf.* **2024**, *158*, 107835. [[CrossRef](#)]

23. Zhong, K.; Wang, C.; Luo, Q.; Zhang, Z.; Zheng, J. Experimental study of a novel guided sequential immersion cooling system for battery thermal management. *Appl. Therm. Eng.* **2024**, *257*, 124337. [[CrossRef](#)]
24. Kalkan, O. Immersion cooling of a cylindrical battery module: An optimum configuration using CFD, NSGA-II and desirability function approach. *J. Energy Storage* **2024**, *100*, 113717. [[CrossRef](#)]
25. Li, Y.; Bai, M.; Zhou, Z.; Lv, J.; Hu, C.; Gao, L.; Peng, C.; Li, Y.; Li, Y.; Song, Y. Experimental study of liquid immersion cooling for different cylindrical lithium-ion batteries under rapid charging conditions. *Therm. Sci. Eng. Prog.* **2022**, *37*, 101569. [[CrossRef](#)]
26. Cao, X.; Shi, Q.; Liu, Q.; Liu, M.; Xiong, C.; Peng, B.; Cao, C.; Wang, X.; Chen, Y.; Cheng, Q.; et al. Full-scale simulation of a 372 kW/372 kWh whole-cluster immersion cooling lithium-ion battery cluster and battery thermal management system design. *Case Stud. Therm. Eng.* **2024**, *63*, 105377. [[CrossRef](#)]
27. Li, Y.; Bai, M.; Zhou, Z.; Wu, W.; Wei, L.; Hu, C.; Liu, X.; Gao, S.; Li, Y.; Song, Y. Thermal management for the prismatic lithium-ion battery pack by immersion cooling with Fluorinated liquid. *Appl. Therm. Eng.* **2024**, *257*, 124453. [[CrossRef](#)]
28. Li, C.; Wang, Y.; Sun, Z.; Wen, X.; Wu, J.; Feng, L.; Wang, Y.; Cai, W.; Yu, H.; Wang, M.; et al. Two-phase immersion liquid cooling system for 4680 Li-ion battery thermal management. *J. Energy Storage* **2024**, *97*, 112952. [[CrossRef](#)]
29. An, Z.; Liu, H.; Gao, W.; Gao, Z. Cooling and preheating performance of dual-active lithium-ion battery thermal management system under harsh conditions. *Appl. Therm. Eng.* **2024**, *242*, 122421. [[CrossRef](#)]
30. Liu, Y.; Aldan, G.; Huang, X.; Hao, M. Single-phase static immersion cooling for cylindrical lithium-ion battery module. *Appl. Therm. Eng.* **2023**, *233*, 121184. [[CrossRef](#)]
31. Liu, J.; Ma, Q.; Li, X. Numerical study on heat dissipation performance of a lithium-ion battery module based on immersion cooling. *J. Energy Storage* **2023**, *66*, 107511. [[CrossRef](#)]
32. Choi, H.; Lee, H.; Kim, J.; Lee, H. Hybrid single-phase immersion cooling structure for battery thermal management under fast-charging conditions. *Energy Convers. Manag.* **2023**, *287*, 117053. [[CrossRef](#)]
33. Hemavathi, S.; Thiru Kumaran, A.; Srinivas, S.; Prakash, A. Synthetic ester-based forced flow immersion cooling technique for fast discharging lithium-ion battery packs. *J. Energy Storage* **2024**, *97*, 112852. [[CrossRef](#)]
34. Satyanarayana, G.; Ruben Sudhakar, D.; Muthya Goud, V.; Ramesh, J.; Pathanjali, G. Experimental investigation and comparative analysis of immersion cooling of lithium-ion batteries using mineral and therminol oil. *Appl. Therm. Eng.* **2023**, *225*, 120187. [[CrossRef](#)]
35. Suresh Patil, M.; Seo, J.; Lee, M. A novel dielectric fluid immersion cooling technology for Li-ion battery thermal management. *Energy Convers. Manag.* **2021**, *229*, 113715. [[CrossRef](#)]
36. Li, Y.; Zhou, Z.; Hu, L.; Bai, M.; Gao, L.; Li, Y.; Liu, X.; Li, Y.; Song, Y. Experimental studies of liquid immersion cooling for 18650 lithium-ion battery under different discharging conditions. *Case Stud. Therm. Eng.* **2022**, *34*, 102034. [[CrossRef](#)]
37. Kong, D.; Peng, R.; Ping, P.; Du, J.; Chen, G.; Wen, J. A novel battery thermal management system coupling with PCM and optimized controllable liquid cooling for different ambient temperatures. *Energy Convers. Manag.* **2020**, *204*, 112280. [[CrossRef](#)]
38. Han, J.; Garud, K.S.; Hwang, S.; Lee, M. Experimental Study on Dielectric Fluid Immersion Cooling for Thermal Management of Lithium-Ion Battery. *Symmetry* **2022**, *14*, 2126. [[CrossRef](#)]
39. Patil, M.S.; Seo, J.; Panchal, S.; Jee, S.; Lee, M. Investigation on thermal performance of water-cooled Li-ion pouch cell and pack at high discharge rate with U-turn type microchannel cold plate. *Int. J. Heat Mass Transf.* **2020**, *155*, 119728. [[CrossRef](#)]
40. Garud, K.S.; Han, J.; Hwang, S.; Lee, M. Artificial Neural Network Modeling to Predict Thermal and Electrical Performances of Batteries with Direct Oil Cooling. *Batteries* **2023**, *9*, 559. [[CrossRef](#)]
41. Han, J.; Garud, K.S.; Kang, E.; Lee, M. Numerical Study on Heat Transfer Characteristics of Dielectric Fluid Immersion Cooling with Fin Structures for Lithium-Ion Batteries. *Symmetry* **2022**, *15*, 92. [[CrossRef](#)]

Disclaimer/Publisher’s Note: The statements, opinions and data contained in all publications are solely those of the individual author(s) and contributor(s) and not of MDPI and/or the editor(s). MDPI and/or the editor(s) disclaim responsibility for any injury to people or property resulting from any ideas, methods, instructions or products referred to in the content.